2009

Power generation in isolated and regional communities: application of a doubly-fed induction generator based wind turbine

Nishad Mendis
University of Wollongong, nnrm786@uowmail.edu.au

Kashem M. Muttaqi
University of Wollongong, kashem@uow.edu.au

Saad M. Sayeef
saad@uow.edu.au

Sarath Perera
University of Wollongong, sarath@uow.edu.au

Power Generation in Isolated and Regional Communities: Application of a Doubly-fed Induction Generator based Wind Turbine

Nishad Mendis, Kashem M. Muttaqi, Saad Sayeef and Sarath Perera
School of Electrical, Computer Engineering and Telecommunication Engineering
University of Wollongong
Australia
Email:nnrm786@uow.edu.au

***Abstract*—The application of a Doubly Fed Induction Generator (DFIG) as a suitable generating scheme in a remote or isolated communities is presented in this paper. Remote Area Power Supply (RAPS) system, a dummy load and its controller with Energy Storage System (ESS) are identified as the key components. The dummy load is used to absorb the power associated with over generation. The battery storage system is used as a storage buffer which could absorb or release the power into the RAPS system when required. It is also used as a secondary control for the DC link voltage of the back-back converter of the DFIG. The hybrid operation of the DFIG, dummy load, ESS and main load is discussed in relation to the system voltage,frequency and DC link stability. The entire hybrid model has been developed using the SimPowerSystem tool box in MATLAB.**

***Index Terms*—Doubly Fed Induction Generator, Remote Area Power Systems, Dummy load, Battery storage system, Dc link voltage stability.**

I. Introduction

Most rural communities and isolated small islands do not benefit from the main grid supply. Presently, energy demand for such locations are mostly supplied through diesel generation systems. However, the operation of such systems have now become a challenge due to the growing environmental concerns and high operating cost [1]. Instead, a hybrid Remote Area Power Supply (RAPS) system would be an attractive solution. Such power systems consist of several renewable energy sources such as wind, solar and hydro. Depending on the availability of resources, a suitable combination of renewable energy sources can be utilised to form the hybrid RAPS system.

Autonomous wind power systems can be used to meet the increasing electricity demand in remote locations where wind is freely available. However, there are various challenges associated with designing such power systems. In this regard, voltage and frequency are the most important aspects to be controlled. In addition, power quality issues, coordination among different components and cost effectiveness are some of the aspects which are still major subjects of interest. Among the various wind turbine technologies available, the application of the Doubly Fed Induction Generator (DFIG), which is normally used for large scale power generation, is preferred [2]. The converters of this topology are only required to be rated at 20-30% of the total capacity of DFIG. Other major advantages of a DFIG scheme include its ability to generate power in both super and sub synchronous speeds, independent control of both active and reactive power, control of power factor, reduced stresses on the mechanical structure and reduction of acoustic noise [3].

Up to now detailed modelling and application of the DFIG for remote operation has been considered only as a stand alone generator. Mathematical modelling of the DFIG for remote application has been discussed in [4]- [6]. In this work a mathematical model of the DFIG and its converter controls are presented employing d-q vector control. Use of other sources in remote area schemes has been stated in scattered literature but little or no modelling or control details are available. As stated earlier, the voltage and the frequency control of the DFIG operating in a remote environment is a major challenge. Also, the generator output has to be independent of the variable shaft speed and loading conditions of the system [5].

The novel hybrid RAPS system considered in this paper which consists of a DFIG (main generator), dummy load and its controller, Energy Storage System (ESS) (ie. battery bank) and main loads is shown in Fig. 1. The various components require careful coordination to achieve the desired voltage and frequency control. In this regard the DFIG system with its controls are closely examined together with supplementary components (dummy load and ESS) and their controls.

The paper is organised as follows. Section II outlines the control methodologies of the DFIG based remote area power system covering (a) Rotor Side Converter (RSC) and (b) Line Side Converter (LSC). Section III discusses the control methodology adopted for the dummy load controller and ESS. Response of the RAPS system for (a) resistive variable load and (b) pump load is discussed in Section IV. Section V examines the suitability of the proposed ESS in relation to DC link voltage stability. Conclusions are given in Section VI.

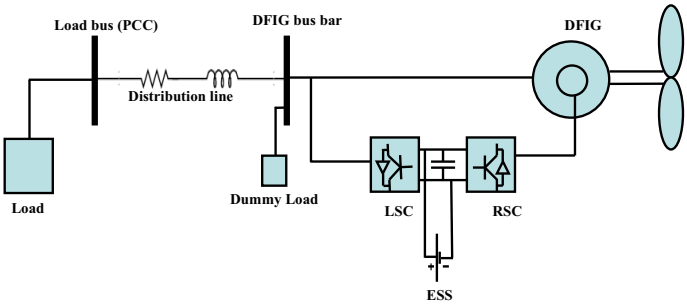

Fig. 1. DFIG based RAPS system with ESS unit

II. Control of Voltage and Frequency for Stand-alone DFIG System

Voltage and frequency control of a stand alone DFIG is quite challenging as it is connected to a weak system. The voltage and frequency control of the machine has to be realised using the RSC controller. However, as stated above, the voltage and frequency of the DFIG should be independent from the load conditions as well as the rotational speed of the machine. The LSC is used to control the DC link voltage and should be able to provide any reactive power to the system if necessary.

In this work the DFIG is modelled in the d-q reference frame with a view to investigate the behaviour of the proposed RAPS system. Vector control is applied to both the RSC and LSC. The mathematical model of the DFIG in an arbitrary rotating reference frame described in [5] is employed in the current work. A Phase Locked Loop (PLL) is used to define the frequency of the RAPS system and the orientation angles for the RSC and LSC. The RSC employs the Indirect Stator Flux Orientation (ISFO) scheme and the LSC employs the Indirect Stator Voltage Orientation (ISVO) scheme for its converter control. The angle difference between the two orientation schemes is always maintained as $\frac{\pi}{2}$.

A. Rotor Side Controller (RSC)

The equivalent circuit of a DFIG in the d-q reference frame with the ISFO can be represented as in Fig. 2. It can be seen that the air gap voltage of the machine appears as the stator voltage if the stator resistance of the machine is neglected. Decoupled control of active and reactive power can be achieved using ISFO for the RSC as mentioned in [5]. With this orientation scheme, the total reactive power of the DFIG can be established using (1) - (4). It is evident that this reactive power consists of two components. The no load reactive power of the DFIG (ie. Q_{mag}) given by (5) is used for magnetisation purposes. The other component (6) which is given by Q_{gen} is used to satisfy the reactive power requirements of the system loads (ie. inductive loads) [6]. With the adopted control strategy, Q_{mag} can be compensated by imposing the condition given by (7). The advantage of the adopted control strategy is that it controls the d-component of rotor current (ie. i_{rd}) in (3), while providing additional VAR requirement which may arise due to the presence of reactive loads. However, the reactive power capability of DFIG through RSC is limited due to the machine characteristics. A typical droop characteristic of the DFIG is shown in Fig. 3 [7]. To enhance the voltage control, the LSC has been modified to provide additional reactive power. Further details are given in section II-B.

The frequency control of the machine should be made independent of the rotational speed and load fluctuations. Hence, the active power component given by (8) cannot be used to develop a control strategy for frequency regulation of the system as it is directly related to the torque of the machine. Generally in the grid connected mode of operation, the q-component of current, i_{rq}, is used to extract the maximum power from wind using the torque reference. In contrast, when the DFIG operates in stand alone mode, i_{rq} should be used to regulate the frequency. Indirectly, the condition given by (9) is used to impose the RSC into the ISFO mode which ensures the system frequency. The frequency control strategy is implemented using the condition given by (10). The proper alignment of the actual orientation angle to the virtual orientation angle defined by PLL ensures a well regulated frequency of operation.

$$Q_s = -\frac{3}{2}V_{sq}i_{sd} \quad (1)$$

$$Q_s = \frac{3}{2}[-\frac{V_s^2}{\omega L_s} + V_s\frac{L_m}{L_s}i_{rd}] \quad (2)$$

$$i_{rd} = i_{rd\ gen} + i_{mag} \quad (3)$$

$$Q_s = Q_{mag} + Q_{gen} \quad (4)$$

$$Q_{mag} = \frac{3}{2}[-\frac{V_s^2}{\omega L_s} + V_s\frac{L_m}{L_s}i_{rd\ mag}] \quad (5)$$

$$Q_{gen} = \frac{3}{2}V_s\frac{L_m}{L_s}i_{rd\ gen} \quad (6)$$

$$i_{mag} = \frac{V_S}{\omega L_m} \quad (7)$$

$$P_s = \frac{3}{2}V_{sq}i_{sq} \quad (8)$$

$$\phi_{sq} = L_s i_{sq} + L_m i_{rq} = 0 \quad (9)$$

$$i_{rq} = -\frac{L_s}{L_m}i_{sq} \quad (10)$$

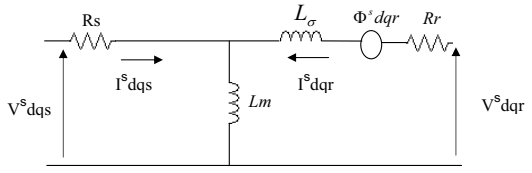

Fig. 2. ISFO equivalent circuit of a DFIG

B. Line Side Controller (LSC)

The main objective of the line side converter controller is to ensure a regulated DC link voltage regardless of magnitude and direction of rotor power. The DC link capacitor of the back-to-back converter acts as a temporary energy storage and

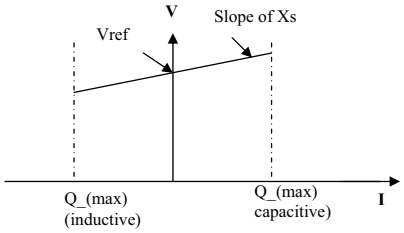

Fig. 3. Wind turbine V-I characteristics

decouples the RSC from the LSC the control systems to a large extent. With ISVO the active power and reactive power of the LSC can be expressed using (11)-(12) respectively. It can be seen that the d-component of the stator current can be used to control the active power and hence the DC link voltage of the system. The reactive power is controlled using the q-component of the stator current. In this paper, the reference q-component of stator current is determined using two control stages. The first stage uses the stator voltage error to determine the reference reactive power for the LSC, which is used by the second stage to produce the q-component of stator reference current.

$$P_s = \frac{3}{2} v_{ds} i_{ds} \quad (11)$$

$$Q_s = \frac{3}{2} v_{ds} i_{qs} \quad (12)$$

III. Auxiliary System components and their control systems

When a DFIG is supplying an isolated load, it is essential to maintain the energy balance of the system to avoid unwanted voltage and frequency fluctuations. In this regard, a dummy load and ESS can be used as supplementary components in the RAPS system. A dummy load can be used to absorb the additional power associated with the system. Any excessive power in the system would cause an increase in the system frequency, which can be used to develop the control strategy for the dummy load controller. An ESS could be used to store available additional energy or provide power if there is a deficit in the system. A battery bank is used as the ESS which is incorporated into the DC link through a bi-directional buck-boost DC/DC converter. The energy balance for the proposed RAPS system can be expressed as in (13).

$$P_{DFIG} = P_{load} \pm P_{battery} + P_{dummy} \quad (13)$$

where,
P_{DFIG}- total power output of DFIG, P_{load}- load demand the DFIG, $P_{battery}$- battery power and P_{dummy}- dummy power

A. Dummy load and its Controller

The condition under which the dummy load operates is given by (14). When the DFIG operates in a remote environment frequency excursions are imminent due to misalignment of the orientation schemes as stated in section II-B. Therefore additional care has been taken to ensure that the dummy load responds only to the change in frequency, Δf, which arises due to the power imbalance associated with the system. A PLL is used to measure the actual system frequency. The frequency error is then compensated through a PID controller. The dummy load consists of a series of resistors which are connected across switches. The resistors operate at voltage zero crossings to ensure minimum level of distortion. A simplified control structure of the dummy load controller is shown in Fig. 4 [8].

$$\Delta f > 0 \quad (14)$$

where,
Δf-frequency deviation of the system

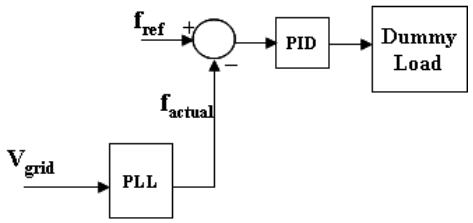

Fig. 4. Dummy load controller

B. Energy Storage System

An energy storage system in a wind farm acts as a load or source depending on the condition of the system. However, the selection of the ESS should be carried out based on the level of uncertainty associated with the system. It is stated in [9] that, an ESS for wind energy applications requires a large storage capacity to absorb power surges resulting from gusts, voltage dips (eg. due to an induction motor starting or faults) and deep wind fluctuations which lasts for seconds or longer. In this paper, a battery storage system has been chosen as the preferred ESS and incorporated into the DC link of the converter system. The estimation of the rating of the battery is extremely site specific. The capacity of the battery bank for the current application is estimated to provide the slip power for 5 minutes in case of an emergency. Equation (15) [9] has been used to estimate the battery capacity. The DC link voltage variation of the back-to-back converter system indirectly provides information regarding the power imbalance of the system. This concept has been used to design the control strategy for the battery system as shown in Fig. 5.

$$E_{battery} = 0.2 P_{rated} t \quad (15)$$

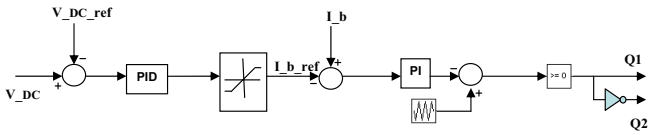

Fig. 5. Control strategy for the battery storage system

IV. RESPONSE OF THE REMOTE AREA POWER SYSTEM WITH DFIG BASED WIND TURBINE

The RAPS system in Fig. 1 has been studied to examine its performance under variable load conditions. Two scenarios have been considered.

- I : The DFIG response for a variable resistive load
- II : Pump load connection

The capacity of the wind plant under rated wind condition (ie. 11 m/s) is 700 kW. In both scenarios, initially the DFIG is supplying power to a 540 kW resistive load. To examine the first scenario, a 160 kW resistive load is switched into the system at t = 4.5 seconds. A 160 kW pump load is connected to the system at t = 4.5 seconds to examine the simulated behaviour for the second scenario.

A. DFIG Response to a variable resistive load

The response of the DFIG system with a variable resistive load is shown in Fig. 6. As stated above, the DFIG is initially supplying a 540 kW load. A 160 kW resistive load is added to the system at t = 4.5 seconds so that the system supplies the rated load of 700 kW. Fig. 6-(a) shows the turbine speed which corresponds to a super synchronous speed of 1.2 pu. The system voltage at Point of Common Coupling (PCC) is shown in Fig. 6-(b). The magnitude of the voltage is regulated at 1 pu $\pm$ 2%. This variation can be justified using (16) [10].

$$\frac{\Delta V}{V} = RP + XQ \tag{16}$$

where,
ΔV- voltage fluctuation, P- total active power output , Q- total reactive power output, R-line resistance and X-line reactance

Equation (16) explains the voltage excursions resulting from the output of a wind generator. In addition, it is assumed that the stator flux orientation is similar to grid flux orientation by neglecting the effect of stator resistance R_s in Fig. 2. As a result, the stator voltage is not compensated for the voltage drop across the stator resistance. Also, the system voltage is regulated by controlling the magnetising current which is highly non-linear. All factors stated above contribute to a distorted voltage and voltage fluctuations. The simulated behaviour of the voltage is not seen to be affected by the resistive step load increase at t = 4.5 seconds. The frequency of the system is shown in Fig. 6-(c), which approximately stays within ± 0.2 Hz. As stated above, the system frequency is mainly controlled by ensuring proper orientation schemes applied to the RSC and LSC. The system frequency and virtual orientation angles are defined using a PLL. The actual orientation angles for RSC and LSC should be determined using the line voltages. However, the system voltage is highly affected by power quality parameters (ie. harmonics, voltage unbalance and flicker). Hence, a proper alignment between actual and virtual orientation angles cannot be expected. This misalignment causes frequency excursions in the system. Upon close examination, it could be identified that there is a close correlation between the frequency and the dummy load power consumption of the system, as seen in Fig. 6-(f). Frequency excursions are quite intense at high peaks of dummy load power. This type of frequency excursion can be expressed using (17). The term ΔP here represents the instantaneous power variation in the RAPS systems which mainly comprises of dummy load power consumption and wind power fluctuations. The frequency of the system is not seen to be influenced by the step change of the resistive load. This can be realised using (10). The frequency regulation can be achieved when $\frac{i_{rq}}{i_{sq}} = \mid \frac{L_s}{L_m} \mid$. During the step increment, both i_{rq} and i_{sq} have increased in equal proportions while satisfying the $\mid \frac{L_s}{L_m} \mid$ ratio. Therefore the frequency of the system is not affected by this load change. The DC link voltage of the system is shown in Fig. 6-(d), which is designed to be regulated at 750 V. In addition to the main control loop at LSC for DC link control, an auxiliary control is supplemented using the battery storage system. The function of the battery storage is discussed in section V. During steady operation, the DC link voltage is seen to be 750 $\pm$ 5V. When the 160 kW load is connected at t = 4.5 seconds, it shows a minimum value of 740 V, which corresponds to a 1.3 % drop. Fig. 6-(e) shows the total active power output of the DFIG. The power fluctuation is influenced by two factors mainly from the operation of dummy load and wind turbine. As dummy load power consumption is variable in nature, it represents a significant portion of the total fluctuating component of the power (ie. ΔP). In addition, the fluctuations in mechanical input to the turbine are transmitted over the turbine shaft to the generator which subsequently appear as power fluctuations.

$$\Delta f = \frac{\Delta P}{Ms + D} \tag{17}$$

where,
Δf- frequency deviation, ΔP- active power variation, M- inertia constant, D- load damping constant

B. DFIG Response to an pump load

The response of the RAPS system to the addition of a 160 kW pump load of induction motor type is investigated. Initially the DFIG is supplying a 540 kW resistive load. At t = 4.5 seconds, a 160 kW pump load is directly connected to the system. The corresponding simulated behaviour of the DFIG is depicted in Fig. 7. The system operates at a speed of 1.2

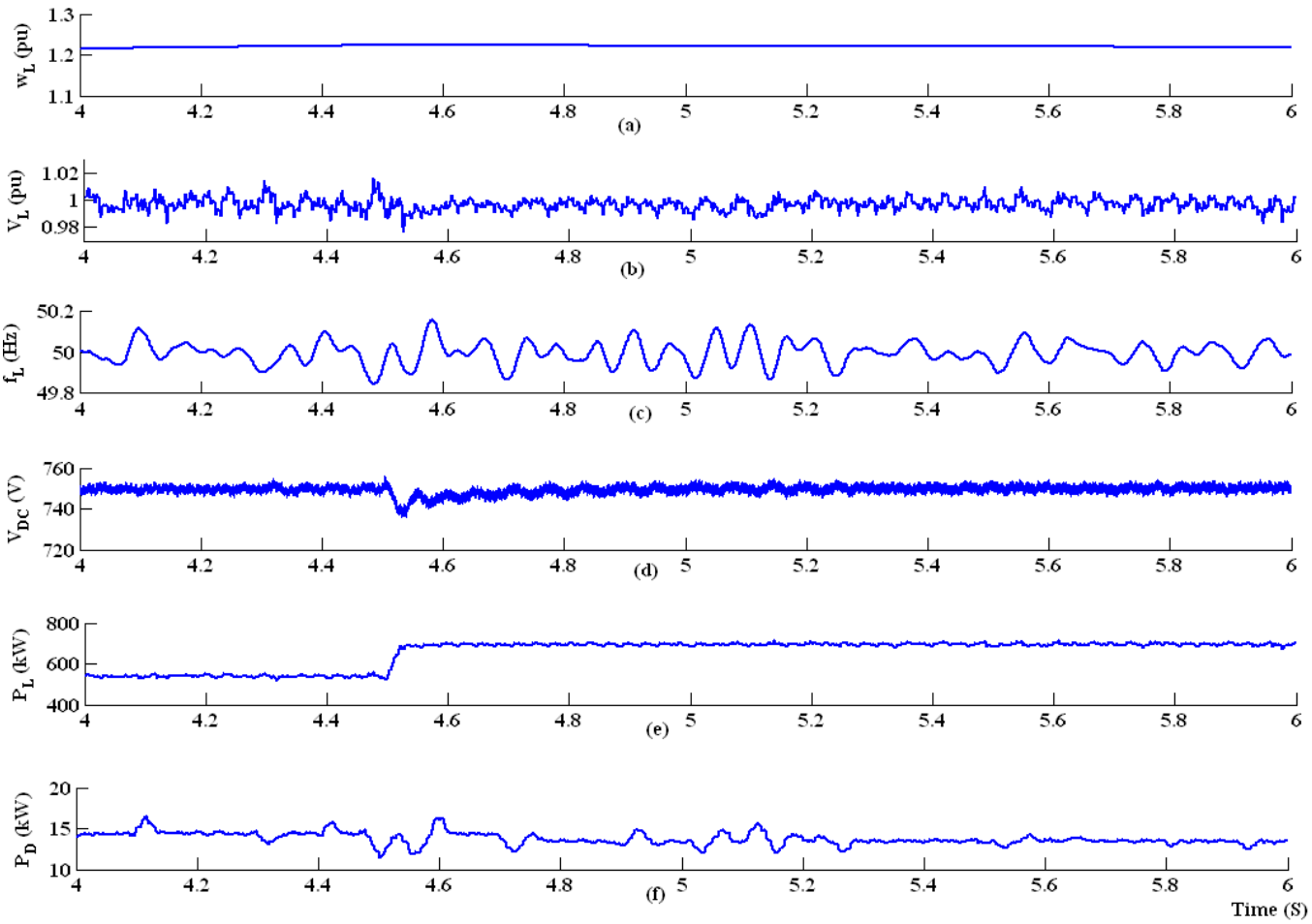

Fig. 6. Responses of the RAPS system at rated wind speed with variable resistive load condition. (a) Turbine mechanical speed, (b) Stator voltage, (c) Stator frequency, (d) DC link voltage, (e) DFIG power output and (f) Dummy load power

pu as shown in Fig. 7-(a). When the pump load is connected to the system, it draws a large current which is essentially reactive as evident from Fig. 7-(f). At this instant, the DFIG is not able to supply the required reactive power which causes the voltage at PCC to drop to a value of 0.65 pu as seen in Fig. 7-(b). The system voltage recovers after 0.25 seconds and is then maintained at its rated value. The frequency of the system is affected by the connection of the pump load but it is regulated within $\pm$ 0.5 Hz. As stated above, to provide the initial reactive power requirement i_{rd} is increased to a high value thus lowering i_{rq} causing the active power to drop as depicted in Fig. 7-(e). This leads to a momentary loss of orientation of the control vectors and to a frequency excursion as seen in Fig. 7-(c). The DC link voltage fluctuates between 695 V and 775 V at the time of pump load connection as depicted in Fig. 7-(d). Further details on the DC link voltage stability in relation to the battery storage system are given in section V.

V. ESS Response to a Pump Load

The operation of a battery bank with the connection of a pump load in a RAPS system is investigated. The standard battery model available in the Simulink tool box has been used for this purpose. The main function of the battery bank is to absorb power from or discharge power into the DC link to maintain a constant DC link voltage. The DC link voltage is seen to fluctuate when there is a power imbalance at the DC link. The voltage variation and the power balance at the DC link capacitor are expressed as in (18) and (19) respectively. Positive battery power indicates discharge of power into the DC link while negative battery power corresponds to power absorbtion from the DC link.

The simulated behavior of the battery bank and DC link voltage are shown in Fig. 8. Initially the system supplies a resistive load of 540 kW. The additional energy available is absorbed by the battery storage system thus keeping the DC link voltage constant as shown in Fig. 8-(b). When the pump load is connected at t = 4.5 seconds, reduction of power caused by reduction of stator voltage leads to additional energy being transmitted into the DC link capacitor. This energy is absorbed by the battery bank to stabilise the DC link voltage as evident from the Fig. 8 -(a) and (b). The battery current varies between $\pm$ 100A at the instant of the pump load connection. After pump load connection, the battery lowers its charging current. A comparison of the DC link stability has been investigated with and without the battery storage system. The DC link voltage without the battery is shown in Fig. 9. It can be seen that the DC link voltage varies between 625 and 825 V when the pump load is connected to the system. This comparison shows the suitability of the proposed control methodology for the battery storage system.

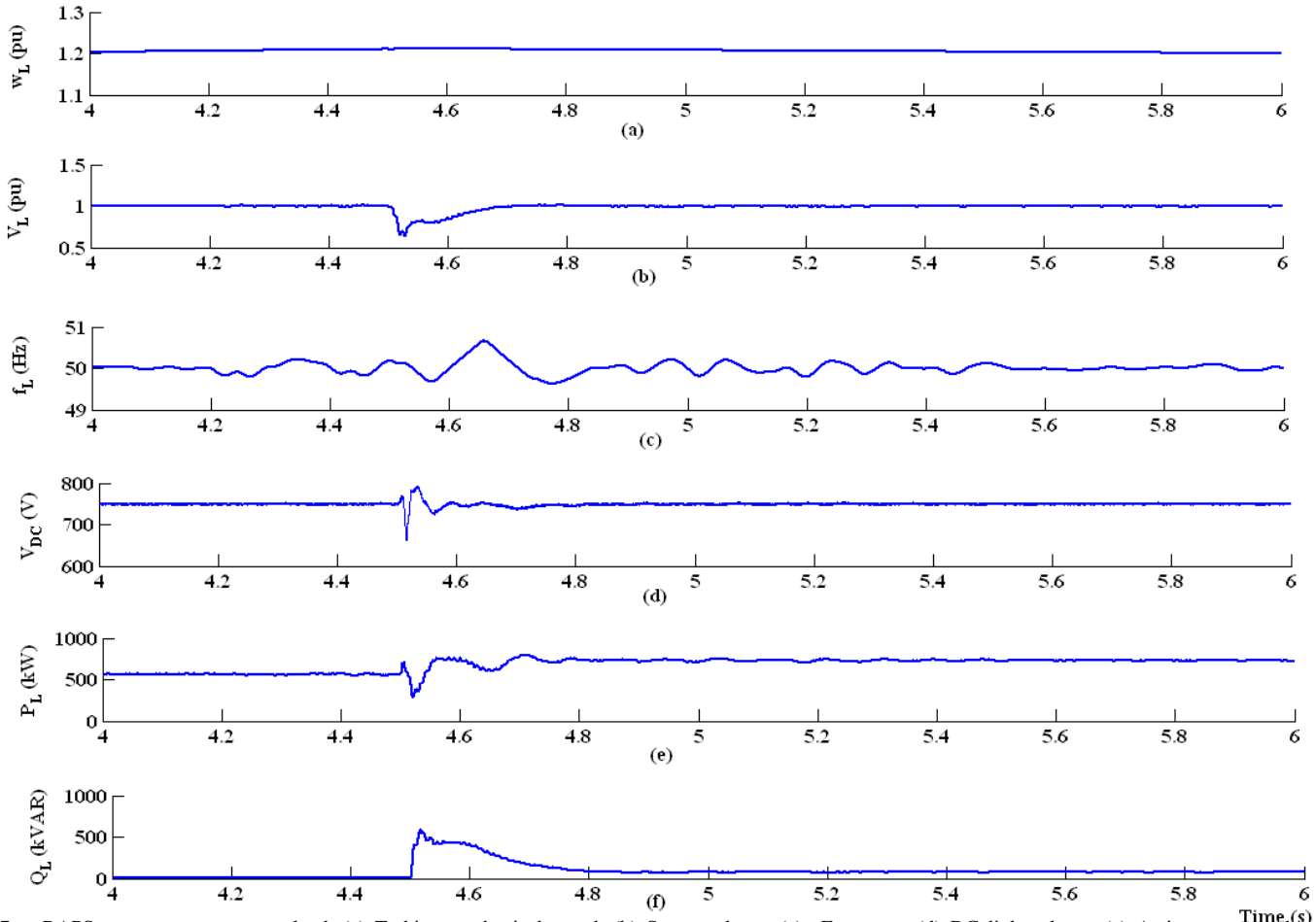

Fig. 7. RAPS responses to a pump load. (a) Turbine mechanical speed, (b) Stator voltage, (c) Frequency (d) DC link voltage, (e) Active power and (f) Reactive power

$$i_c = C\frac{dV}{dt} \tag{18}$$

$$P_{RSC} = P_{LSC} \pm P_{battery} \tag{19}$$

where,
P_{RSC}- RSC power, P_{LSC}- LSC power and $P_{battery}$- battery power

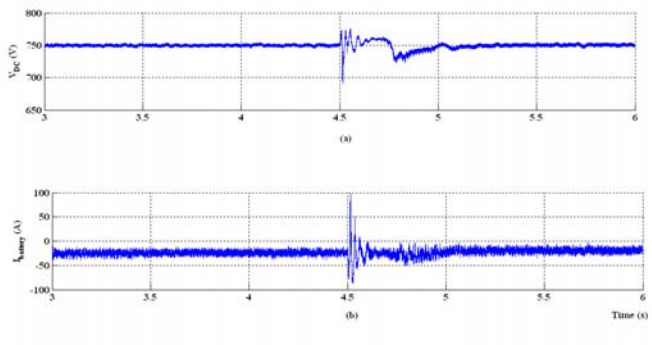

Fig. 8. ESS responses to a pump load. (a) DC link voltage and (b) Battery current

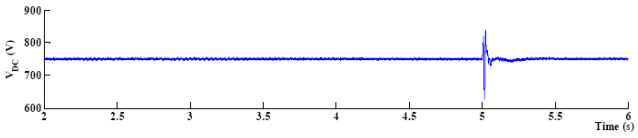

Fig. 9. DC link voltage to a pump load without battery system

VI. Conclusions and Future Work

This paper has investigated the hybrid operation of a DFIG based remote area power system. The system performance was investigated in relation to the bandwidth of the voltage regulation capability under variable load conditions (with resistive load and pump load). It has been identified that the system voltage and frequency regulation are well under control with the variable resistance load alone compared to the case of the connection of pump load. It has been observed that the dummy load makes a considerable contribution to the regulation of the frequency of the system. The proposed battery storage system works effectively throughout the operation. Also, it contributes towards improving transient stability of the DC link. However, the fluctuating nature of the battery current shortens the life of the battery bank. Therefore additional measures have to be taken to prevent the battery bank running into such operation. The authors are currently working on

setting up an experimental test bed consisting of a 7.5 kW DFIG to verify the simulated results.

REFERENCES

[1] T. Senjyu, T. Nakaji, K. Uezato, T. Funabashi, "A Hybrid Power System Using Alternative Energy Facilities in Isolated Island", *IEEE Transaction on Energy Conversion*, vol. 20, issue 2, Jun 2005, pp. 406 - 414.

[2] T.Ackermann and L. Soder "An Overview of Wind Wnergy-Status 2002", *Renew.Sustain Energy Rev.*, vol. 6, Feb./Apr. 2002, pp. 67 - 128.

[3] S. Li, T.A Haskew, "Analysis of Decoupled d-q Vector Control in DFIG Back-to-Back PWM Converter", *Power Engineering Society General Meeting*, 24-28 Jun 2007, pp. 1 - 7.

[4] D. Forchetti, G. Garcia and M. I. Valla, "Vector Control Strategy for a Doubly-Fed Stand-Alone Induction Generator", *28th Annual Conference on Industrial Electronics*, vol. 2, 5-8 Nov. 2002, pp. 991 - 995.

[5] R. Pena, R. Cardenas, G. M. Asher, J. C. Clare, J. Rodriguez and P. Cortes, "Vector Control of a Diesel-Driven Doubly Fed Induction Machine for a Stand-Alone Variable Speed Energy System", *28th Annual Conference on Industrial Electronics*, vol. 2, 5-8 Nov. 2002, pp. 985 - 990.

[6] L. Holdsworth, X.G Wu, J.B Ekanayake and N. Jenkins, "Comparison of Fixed Speed and Doubly-Fed Induction Wind Turbines During Power System Disturbances", *IEE Proceedings, Generation, Transmission and Distribution*, vol. 150, May 2003, pp. 243 - 252.

[7] R. Gangnon, G. Sybille, S. Bernard, D. Pare, S. Casoria and C. Larose, "Modelling and Real-Time Simulation of a Doubly-Fed Induction Generator Driven by a Wind Turbine ", *International Conference on Power Systems Tranisents*, Jun. 2005, pp. 1446 - 1449.

[8] M. Aktarujjaman, M. A. Kashem, M. Negnevitsky and G. Ledwich, "Control Stabilisation of an Islanded System with DFIG Wind Turbine", *1st International Power and Energy Conference, (PECon 2006)*, 28-29 Nov. 2006, pp. 312 - 317.

[9] L. Wei and G. Joos "A Power Electronic Interface for a Battery Supercapacitor Hybrid Energy Storage System for Wind Applications" *Power Electronics Specialists Conference*, 15-19 Jun. 2008, pp. 1762 - 1768.

[10] G. Takata, N. Katayama, M. Miyaku and T. Nanahara "Study on Power Fluctuation Charactersics of Wind Energy Converters with Flcutuating Torque" *Electrical Engineering in Japan*, vol.124-B, Oct. 2004, pp. 1231 - 1239.

ACKNOWLEDGEMENT

This work is supported by the Australian research Council (ARC) and Hydro Tasmania Linkage Grant, LP0669245. The authors gratefully acknowledge the support and cooperation of Hydro Tasmania personnel in providing data and advice on the operation of remote area power supply system.